Experimental and Theoretical Analysis of Subcooling Control in Residential Air Conditioning Systems

Bruno Yuji Kimura de Carvalho
ACRC, the University of Illinois, Urbana, Illinois, USA, brunoykc@illinois.edu

Pega Hrnjak
ACRC, the University of Illinois, Urbana, Illinois, USA

Experimental and Theoretical Analysis of Subcooling Control in Residential Air Conditioning Systems

Bruno Yuji Kimura DE CARVALHO[1]*, Pega HRNJAK[1,2]*

[1]ACRC, University of Illinois at Urbana-Champaign,
Urbana, Illinois, USA
brunoykc@illinois.edu

[2]Creative Thermal Solutions Inc.
Urbana, Illinois, USA
pega@illinois.edu

* Corresponding Author

ABSTRACT

Widespread use of electronic expansion valves in residential air conditioning systems has provided an opportunity to further improve performance by use of alternative refrigerant flow control strategies. This paper focuses on an experimental and theoretical investigation on the effect of subcooling control in air conditioning system. A 2 Ton (7 kW) R410-A system was used in the experimental study and a model for the same system was developed and validated. The paper provides a theoretical analysis and determination of a control scheme to maximize COP and an experimental validation on the performance of a RAC system with subcooling control against a TXV-based baseline system. The theoretical analysis showed that subcooling can be defined as a linear function of temperature difference of refrigerant condensation and condenser air (ΔT_{cra}) and that the effect of the evaporator conditions on its COP-maximizing values are negligible. The system was evaluated at AHRI 240/270 dry conditions with a properly charged TXV (6600g) and EXV subcooling control (8500g) comparison. Results show an average 9.8% increase in COP and 10.4% in capacity using subcooling control for the SEER conditions and a resulting increase of 9.4% in SEER. Validation with both experimental and model data show that subcooling control based on ΔT_{cra} provides a control scheme with good agreement to the data for air conditioning system capable of increasing both COP and capacity.

1. INTRODUCTION

The majority RAC systems rely on superheat control to regulate refrigerant flow and prevent liquid intake at the compressor suction. While this approach provides acceptable performance with relatively low cost it does not fully utilize the evaporator or guarantee maximum efficiency at any condition. An alternative to evaporator superheat-controlled throttling is to regulate the mass flow rate by using condenser subcooling as the control parameter. Pottker and Hrnjak (2015a) have previously shown that controlling subcooling can potentially increase system performance by 2.7%-8.4% in simulations comparing different refrigerants. This increase in system efficiency by controlling subcooling is backed by thermodynamic and thermoeconomic analysis (Sebas, 2006; Pottker and Hrnjak, 2012) showing the existence of a COP-maximizing subcooling, as shown in Fig. 1a and equations 1, 2 and 3. To increase subcooling requires more charge in the condenser which reduces the two-phase heat transfer area in it and raises the condensation pressure, while simultaneously decreasing evaporator inlet enthalpy. These two effects cause an increase in specific compression work and refrigerating effect, respectively. As these opposing effects increase with subcooling a trade-off exists which lead to a maximum COP. Yamanaka et al. (1997) have shown that automotive air conditioning systems can benefit from dedicated subcoolers.

The second benefit of using condenser subcooling as a control variable for the expansion valve is shown in Fig. 1b, which enables operation with no superheat on the evaporator, since this parameter is not used regulate the flow anymore. This allows elimination of dryout in the evaporator and reduction of maldistribution if any is present, which leads to higher heat transfer coefficients and operation at increased evaporation pressures. A significant improvement in COP can be obtained by controlling subcooling with a properly charged system while still operating with a saturated evaporator outlet.

$$COP' \approx COP\left(1+\frac{\Delta q}{q}-\frac{\Delta w}{w}\right) \quad (1)$$

$$COP = \frac{q}{w} \quad (2)$$

$$COP' = \frac{q+\Delta q}{w+\Delta w} \quad (3)$$

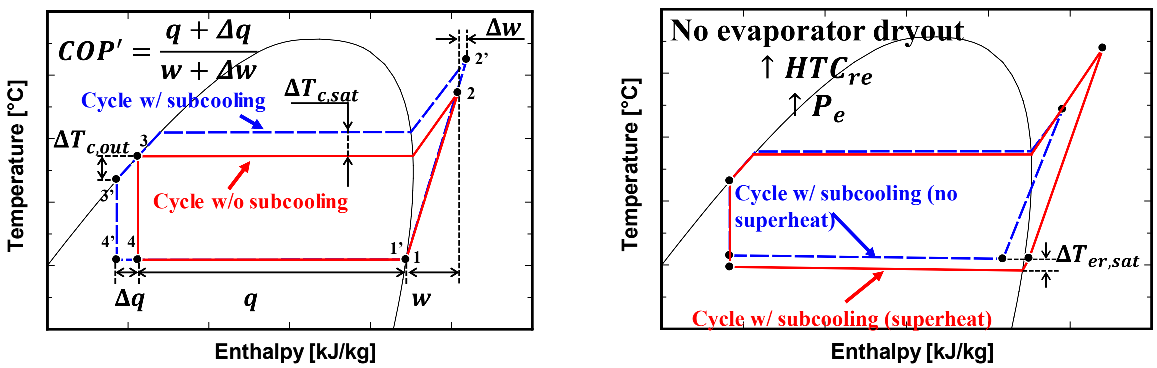

(a) **(b)**

Figure 1: Maximum COP as a balance of w and q increase with subcooling (a) and increased evaporator effectiveness when operating with no superheat and controlling expansion device through subcooling

Pottker and Hrnjak (2015b) also showed that the use of an internal heat exchanger reduces the overall performance improvement from controlling subcooling since it competes towards mitigating throttling losses. Xu and Hrnjak (2014) also investigated the use of subcooling control through a RAC R410-A system showing promising improvements in COP. Pitarch et al. (2017a, b, c) have also studied subcooling control in heat pump water heaters using natural refrigerants and concluded that optimal subcooling may be obtained as a function of the temperature lift of the secondary fluid or a fixed pinch point temperature difference may be used as a simpler control strategy to keep performance close to optimal levels. Experimental results corroborating the benefit from COP-maximizinng subcooling and no evaporator superheat combined were presented by de Carvalho and Hrnjak (2019ab).
This paper will investigate theoretically the use of condenser variables to the COP-maximizing subcooling and experimentally evaluate the impact of subcooling control on the performance of a R410-A air conditioning. A comparison the same system using a thermostatic valve will also be presented along with a comparison of SEER improvements.

2. THEORETICAL ANALYSIS

To understand the performance behavior as a function of subcooling a simple heat exchanger and compressor model was written in EES (Klein, 2020). The model used an ε-NTU single pass crossflow method for the condenser and assumed fixed evaporator outlet quality of 1 and evaporation temperature of 10°C. Compression was initially assumed ideal and the only component modelled was the condenser heat transfer by changing the subcooling and calculating the required heat transfer area on the heat exchanger to provide the given subcooling, while the mass flow rate was calculated to provide the fixed cooling capacity. Table 1 shows the constant variables used in the model to simplify the analysis and the refrigerant used was R410a. Pressure drop across the condenser and evaporator were also neglected.

Table 1: Fixed constants for subcooling control cycle analysis

$HTC_{cr.SC}$	$HTC_{cr.TP}$	$HTC_{cr.SH}$	HTC_{ca}	A_{ca}	A_{cr}	Q_e	T_{cai}	$T_{er.sat}$	x_{ero}
[W m^2 K^{-1}]	[W m^2 K^{-1}]	[W m^2 K^{-1}]	[W m^2 K^{-1}]	[m^2]	[m^2]	[W]	[°C]	[°C]	[-]
900	3050	300	33	33	1	5000	35	10	1

For a given input of subcooling the model solved for the condensation pressure and the heat transfer area used by the superheated, two-phase and subcooling regions. As subcooling increased more heat transfer area was required to cool the single-phase refrigerant which decreased two-phase area, while the superheat area did not see any significant change. The overall refrigerant side HTC is decreased due to a smaller two-phase area which drive the condensation temperature up to compensate for it. Fig. 2 shows the change in normalized subcooling and two-phase areas along with the reduction in normalized two-phase heat transfer on the condenser.

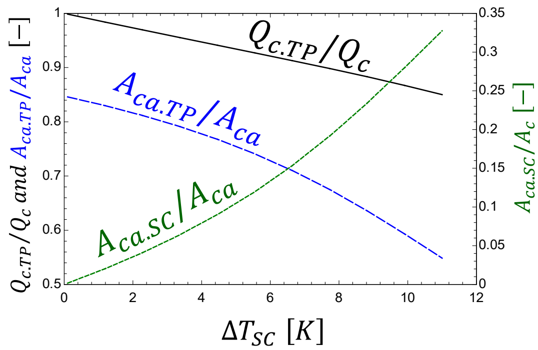

Figure 2: Normalized subcooling/two-phase heat transfer areas and two-phase heat transfer vs condenser subcooling

The increase in condensation temperature overcomes the lower overall refrigerant side HTC by providing a large temperature difference on the condenser. Fig. 3a shows how the condensation to air inlet temperature difference, Eq. 4, increases with subcooling. A higher condensation pressure will result in an increase in specific compressor work while the subcooling reduces evaporator inlet enthalpy boosting specific cooling capacity, as shown in Fig. 3b.

$$\Delta T_{cra} = T_{cr.sat} - T_{cai} \tag{4}$$

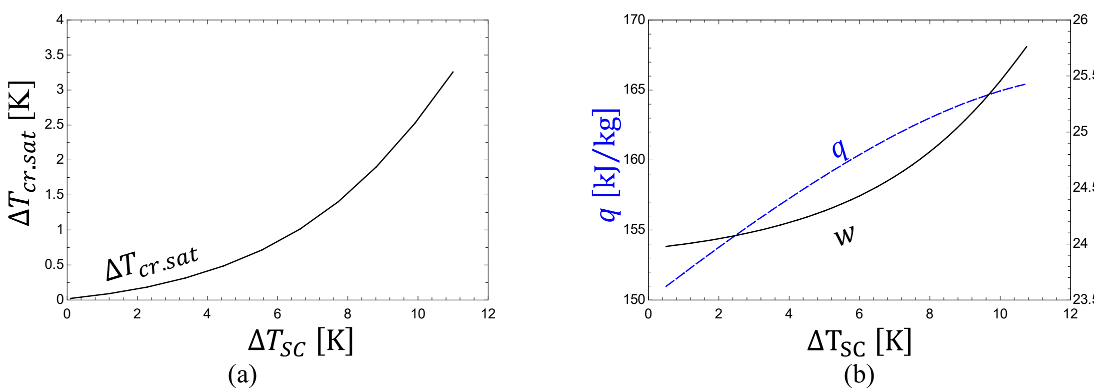

Figure 3: Condensation-air inlet temperature difference (a); specific cooling capacity and compressor work (b) vs condenser subcooling

The different rate of change in specific cooling capacity and compressor work leads to a maximum COP. Also, if the condenser size is varied it also affects how much heat transfer area is required to achieve a certain value of subcooling which in turn changes how the condensation pressure increases with subcooling. Eq. 5 shows how subcooling heat transfer may be calculated, for a smaller condenser ΔT_{cra} will be higher which in turn will required a lower effectiveness, or heat transfer area, to obtain the same subcooling for constant refrigerant heat capacity rate. This drives the COP-maximizing subcooling higher as the condenser is decreased, or the capacity is increased (for a constant condenser size).

$$Q_{SC} = \varepsilon_{SC} \Delta T_{cra} C_{r.SC} \tag{5}$$

Table 2 shows how much normalized subcooling heat transfer area is required to achieve the same amount of subcooling with a fixed cooling capacity of 5 kW for different normalized condenser areas. The subcooling heat transfer area increases with larger condensers meaning two-phase area is sacrificed to obtain the required subcooling.

Table 2: Fixed constants for subcooling control cycle analysis

$A_{ca}/33$ [-]	0.75	1.00	1.25
$A_{ca.SC}/A_{ca}$ @ $\Delta T_{SC} = 5\ K$ [-]	0.099	0.104	0.114

The model shows these effects on the normalized COP vs. subcooling in Fig. 4a and the COP-maximizing subcooling as a function of ΔT_{cra} in Fig. 4b. It is important to note that for reasonable ΔT_{cra} values usually observed in A/C and H/P system COP-maximizing subcooling varies almost linearly with ΔT_{cra}, thus a possible subcooling-based control parameter is a linear function of ΔT_{cra}, shown in Eq. 6.

$$\Delta T_{SC}(COP_{maximizing}) \cong a\Delta T_{cra}\ (K) + b \tag{5}$$

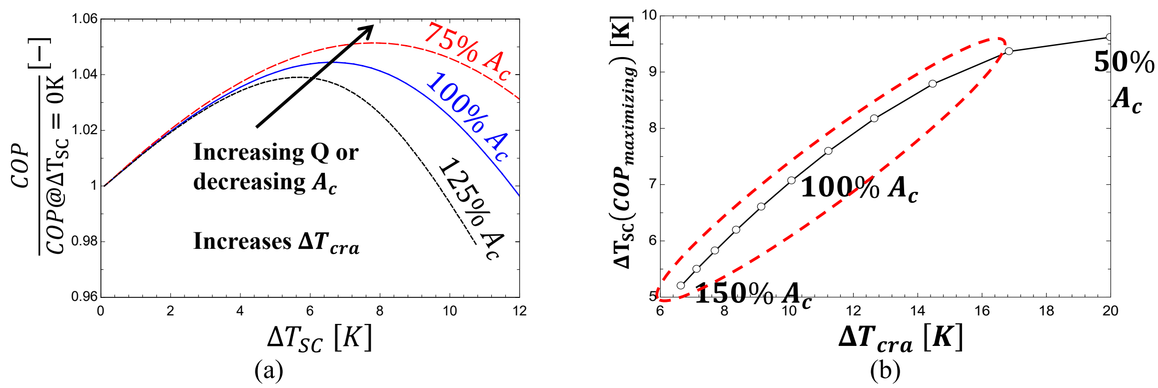

Figure 4: Normalized COP vs. subcooling (a) and COP-maximizing subcooling vs ΔT_{cra} (b)

To evaluate the effect of the evaporator the evaporation temperature was varied from 10C to 5C and 0C, a similar analysis as shown in Fig. 4b was conducted. The effect of evaporation temperature on the COP-maximizing subcooling as a function of ΔT_{cra} is shown in Fig. 5. By decreasing the evaporation temperature, the specific compression work is increased, but with ideal compression the compression curve is constant which leads to lower relative increases in compression work and allows for higher COP-maximizing subcooling. On the other hand, once a real compressor curve is used, in this case an AHRI-540 based 10-coefficient curve fitting of a scroll compressor performance map was used. Once a real compressor polytropic curve is used the effect of the evaporation temperature is mitigated corroborating use of Eq. 5 to define the subcooling control scheme.

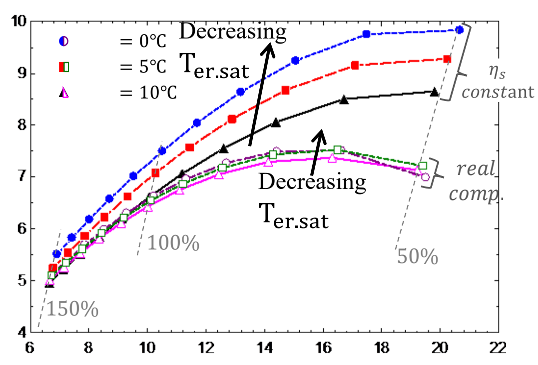

Figure 5: COP-maximizing subcooling vs ΔT_{cra} for ideal and real compressor curves

3. FACILITY

The facility, shown in Fig. 6, is comprised of two environmental chambers that can maintain outdoor and indoor temperatures within ± 0.5°C and absolute humidity ±2%. Each chamber uses a variable speed wind tunnel with electric heaters and cooled glycol heat exchangers to simulate a range of operating conditions. Humidity in the chambers can be controlled through steam injection.

4WV: 4-way valve
ABL: Air blender
ACC: Accumulator
AIR: Air
BL: Blower
CC: Charge compensator
CD: Condenser
CP: Compressor
DP: Differential pressure transducer
DPS: Dew-point sensor
EGC: Ethylene glycol chiller
EGHX: Ethylene glycol heat exchanger
ERH: Electric resistance heater
EV: Evaporator
EXV: Electronic expansion valve
FN: Flow nozzle
MF: Muffler
MFM: Mass flow meter
P: Absolute pressure transducer
SI: Steam injection
T: Type-T thermocouple
TCG: Thermocouple grid
TXV: Thermostatic expansion valve
VFD: Variable frequency drive

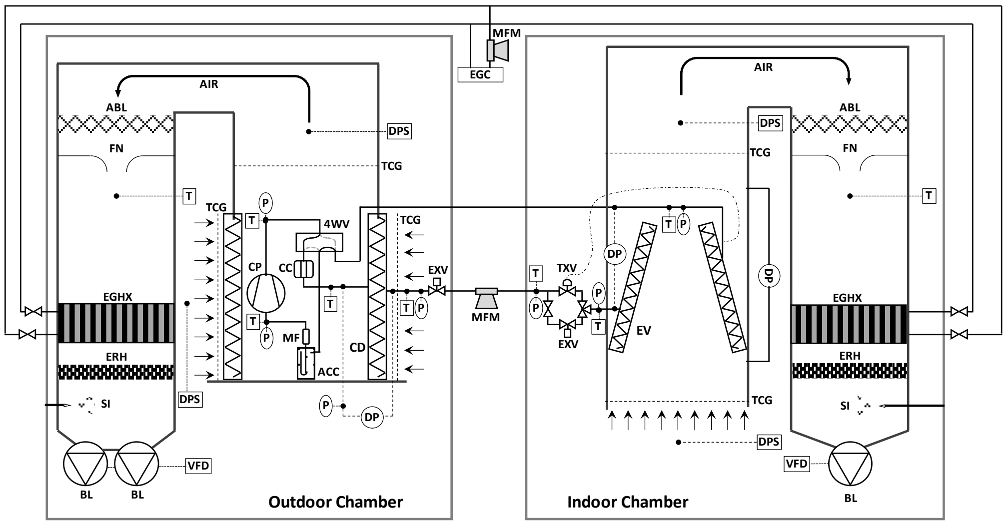

Figure 6: Layout of facility for performance evaluation

The capacity is currently determined by both air side energy balance, and refrigerant side energy balance. The average uncertainty for compressor, heaters and blowers power measurement is within ±0.2%. Air-side and refrigerant side capacity calculations have an expanded uncertainty of around ±4% and COP uncertainty is calculated to be ±5%.
The 2 Ton (7kW) R410-A residential reversible system used has a round-tube A-coil indoor heat exchanger with a thermostatic valve (TXV) and a round-tube horizontal condenser with an electronic expansion valve (EXV) for heat pump operation. Two EXVs were installed in the system in parallel with its present expansion devices to allow subcooling control in both A/C and H/P operation modes. Fig. 7 shows a diagram of the system cycle only. Table 3 shows the specifications for the heat exchangers on the outdoor and indoor chamber.

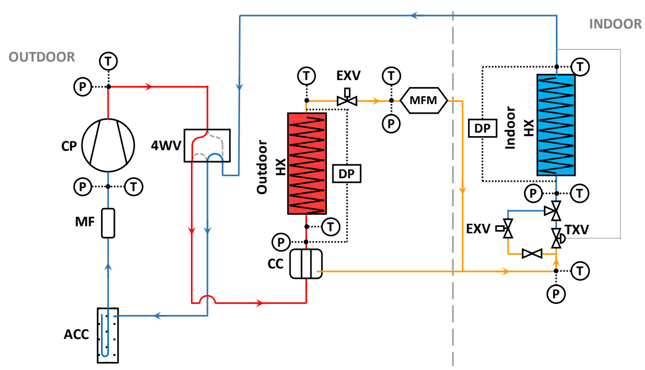

Figure 7: Schematic drawing of the air-conditioning system evaluated

Table 3: Residential system heat exchanger specifications

	Outdoor heat exchanger	Indoor heat exchanger
Description	2 rows, 8 circuits, 20 fpi	2 slabs, 3 staggered rows, 8 circuits, 14.5 fpi
Face area	2.81 m^2 (30.25 sqft)	0.689 m^2 (7.42 sqft)
Core depth	0.038 m	0.056 m
Core volume	0.1068 m^3	0.03858 m^3
Air side area	153.53 m^3	40.1 m^3
Refrigerant side area	4.61 m^3	2.39 m^3
Material	Aluminum fins, copper tubes, vapor line O.D. = 22 mm, liquid line O.D. = 9.5 mm	

4. EXPERIMENTAL RESULTS

4.1 Test conditions

Improvement in SEER provided by subcooling control was evaluated based on AHRI 210/240, but at dry conditions, and the baseline uses the original system thermostatic valve with the nominal charge of 6600g. Subcooling was controlled by bypassing the flow through an electronic expansion valve. The charge selection was done by running the system at the maximum A/C compressor speed of 53.33 Hz, 40C outdoor air temperature and 26.67C indoor air temperature to obtain the COP-maximizing subcooling while still having no superheat on the evaporator, this would ensure the use of the accumulator as a charge receiver at lower loads. The charge obtained for subcooling control was of 8500g or 1100g higher than the nominal charge. Minimum load conditions were run at a compressor speed of 30 Hz and the default degradation coefficient of 0.20 was used. Outdoor air flow rate was kept at 1.085 m^3s^{-1} (2300 CFM) while indoor air flow rate was 0.425 m^3s^{-1} (900 CFM) for full capacity and 0.236 m^3s^{-1} (500 CFM)

4.2 Subcooling control effect on system performance

By controlling subcooling a COP-maximizing subcooling was achieved for all four conditions required for the SEER calculation. Fig. 8ab show the COP as a function of subcooling comparing the subcooling controlled system with the thermostatic valve properly charged for conditions A_{Full} and A_{Low}. Due to the large condenser in the system used for this study the required subcooling for maximum COP is very low at partial load conditions. COP improvement is of 13.2% and 10.9% for maximum and minimum capacities, respectively, due to the improved evaporator performance. Fig. 9 shows the T-h diagram comparing the COP-maximizing subcooling point and the thermostatic valve with its proper charge. If a thermostatic valve or fixed expansion system is charged correctly it should operate at near COP-maximizing subcooling as the charge controls the subcooling for the system under a specific condition. The TXV-based system does not deviate from the COP-maximizing subcooling, indicating that most of the benefit in COP for subcooling control comes from the better performing evaporator in this case. The COP improvement obtained for conditions B_{Full} and B_{Low} was of 9.7% and 5.5%, respectively, showing that improvements vary per condition.

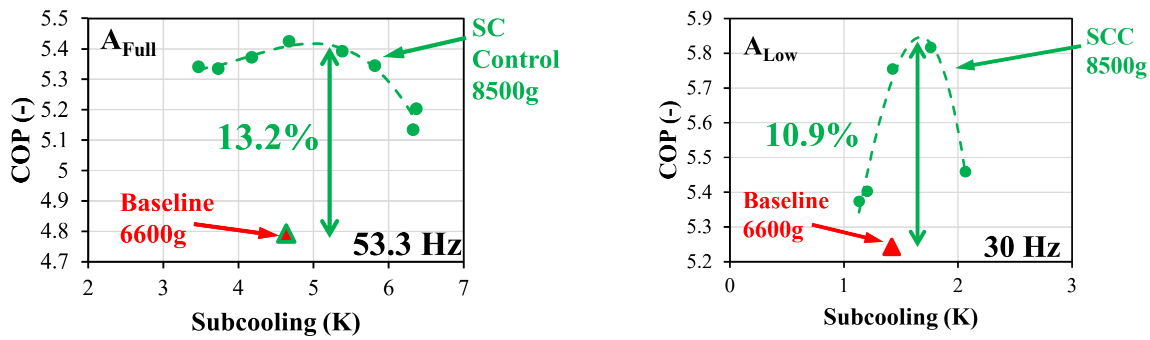

(a) (b)

Figure 8: Subcooling control and TXV-based system performance at condition A_{Full} (a) and A_{Low} (b)

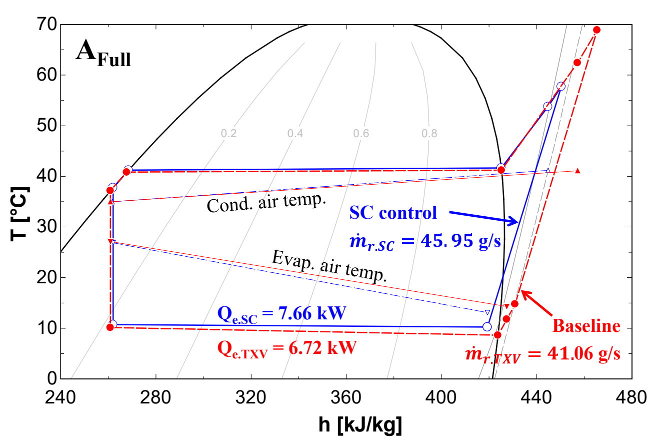

Figure 9: T-h diagram comparing SC control and TXV-based system performance in A_{Full} condition

4.3 SEER improvement from subcooling control

By using the four data points of A_{Full}, A_{Low}, B_{Full}, B_{Low} the SEER can be calculated and it is shown in Fig. 10. The increase in capacity for the low load conditions is not beneficial for SEER because it increases losses due higher degradation with more frequent on/off cycling. Nevertheless, SEER is improved by 9.4% and the capacity increase could be used to allow for smaller compressor that could still meet the required loads thus decreasing system cost. If a compressor with broader frequency control range was employed cycling degradation effect could be mitigated and the increased capacity could be used when necessary. Operation with no evaporator superheat also decreases discharge temperatures (more than 10 K as shown in Fig. 9) leading to easier operation for R32 system which are known to have high compressor outlet temperatures.

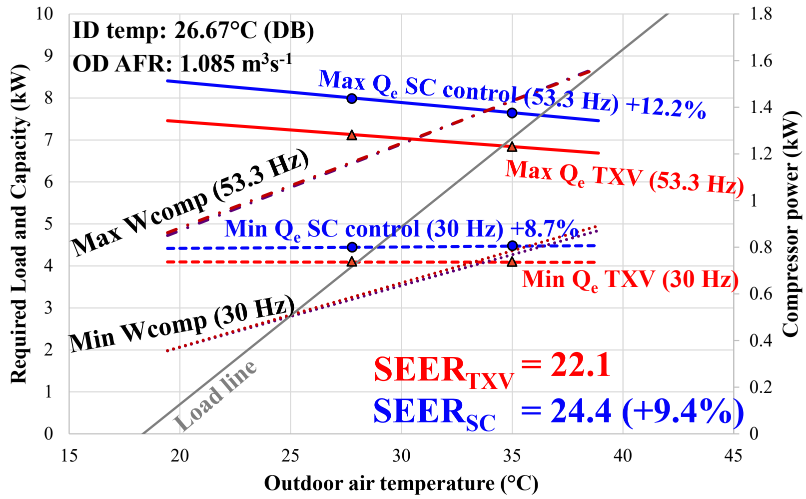

Figure 10: Load, capacity and compressor power vs outdoor air temperature for SEER representation

4.4 Subcooling control scheme

As previously shown in section 2 the theoretical analysis indicates that it is possible define the COP-maximizing subcooling as a linear function of ΔT_{cra}. To define this function the experimental data set from the SEER tests along with data sets for other A/C conditions, data from Xu and Hrnjak (2014) for a similar system and a python-based model data written based on the system used in this investigation were combined to better develop the linear regression for the control curve. Fig. 11 shows the final curve obtained along with the ΔT_{cra} for the 4 experimental points used in the SEER calculation. All experimental and model data agree with the linear regression with an R^2 of 98.17%, and the regression was defined for ΔT_{cra} of up to 14 K. These results further validate the theoretical analysis, but its application must be experimentally tested with a different system along with modeling using different compressors, heat exchangers and accumulators to better understand the effect of other components on this control scheme.

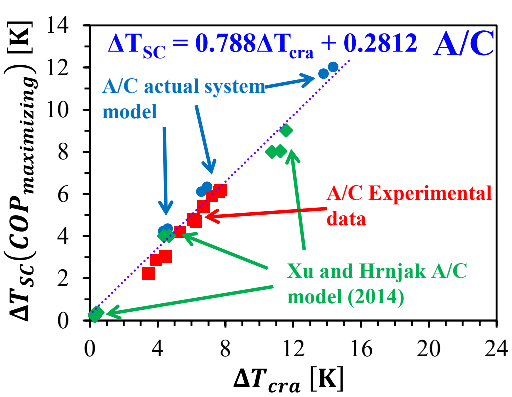

$$\Delta T_{cra.A_{Full}} = 6.6\ K$$
$$\Delta T_{cra.A_{Low}} = 3.9\ K$$
$$\Delta T_{cra.B_{Full}} = 6.6\ K$$
$$\Delta T_{cra.B_{Low}} = 3.7\ K$$

Figure 11: Control curve based on linear regression of the COP-maximizing subcooling as a function of ΔT_{cra} and values for SEER points

6. CONCLUSIONS

This paper presented a theoretical and experimental analysis of subcooling control on a residential air conditioning system. The theoretical analysis obtained a simple linear curve for the COP-maximizing subcooling as a function of ΔT_{cra}, with very little effect from the evaporator condition which is mitigated by the polytropic curve of the compressor. An off-the-shelf residential air conditioning system was used to evaluate the overall COP and SEER improvement when using subcooling control over the same system with a TXV. Results show that if a system is properly charge it can achieve close to COP-maximizing subcooling even with a TXV, but the ability to operate with no superheat on the evaporator outlet while still controlling subcooling to maximize efficiency provided an improvement in COP of approximately 9.8% and a SEER improvement of 9.4%. The SEER increase is penalized by the cycling degradation due to the average increased capacities of 10.4% which require more often on/off cycling on the low load conditions.

The experimental and model results for the system used in this study along with another author's data for a similarly sized system show very good agreement with the control scheme obtained by the theoretical analysis corroborating the single strong relation between ΔT_{cra} and COP-maximizing subcooling. Further investigation on how each component may change the subcooling control strategy as well as a study on the robustness of this control, especially considering how partial load conditions required very low subcooling which increases measurements uncertainties, must be carried out.

The use of a linear regression curve to control COP-maximizing subcooling based on ΔT_{cra} allowing operation with no superheat while keeping the system at a stable condition has shown to be a promising alternative to TXV or fixed expansion air conditioning systems.

NOMENCLATURE

The nomenclature should be located at the end of the text using the following format:

A	Heat transfer area	(m^2)
AFR	Air volumetric flow rate	($m^3\ s^{-1}$)
A/C	Air conditioning	
AFR	Air flow rate	(m^3 s-1)
C	Heat capacity rate	(kJ K^{-1})
COP	Coefficient of performance	(–)
EXV	Electronic expansion valve	
ε	Effectiveness	(-)
h	Enthalpy	(kJ kg-1)
ID	Indoor	
H/P	Heat pump	
HTC	Heat transfer coefficient	(W $m^{-2}\ K^{-1}$)
m	Mass flow rate	(kg s-1)
OD	Outdoor	
P	Pressure	(kPa)
q	Specific cooling capacity	(kW kg^{-1})
Q	Capacity	(kW)
RAC	Residential air conditioning	
SC	Subcooling	
SEER	Seasonal energy efficiency ratio	
SH	superheat	
T	Temperature	(°C or K for differences)
TXV	Thermostatic expansion valve	
x	Refrigerant quality	(-)
w	Specific work	(kW kg-1)
W	Work/Power	(kW)

Subscript

a	air (subscript)
c	condenser (subscript)

comp	compressor (subscript)
e	evaporator (subscript)
i	inlet (subscript)
o	outlet (subscript)
r	refrigerant (subscript)
sat	saturation (subscript)
SC	subcooling (subscript)
SH	superheat (subscript)
TP	two-phase (subscript)

REFERENCES

de Carvalho, B.Y.K., Hrnjak, P. (2019). Performance Characteristics of a Residential Air Conditioning System with Subcooling Control. *Proceedings of the 25th International Congress of Refrigeration, Montreal, Canada* (1135). Paris, France: IIF/IIR

de Carvalho, B.Y.K., Hrnjak, P. (2019). Performance Evaluation and Strategies of Subcooling Control in Residential Heat Pump Systems. *Proceedings of the 25th International Congress of Refrigeration, Montreal, Canada* (1159). Paris, France: IIF/IIR

Feng, L., Hrnjak, P. (2016). Experimental and Numerical Study of a Mobile Reversible Air Conditioning-Heat Pump System. *Proceedings of the 16th International Refrigeration and Air Conditioning Conference at Purdue, West Lafayette*, *USA* (2569). West Lafayette, USA. Purdue University.

Pitarch, M., Navarro-Peris, E., Gonzalvez-Macia, J., Corberan, J.M. (2017a). Experimental study of a subcritical heat pump booster for sanitary hot water production using a subcooler in order to enhance the efficiency of the system with a natural refrigerant (R290). *International Journal of Refrigeration, 73, 226-234.*

Pitarch, M., Navarro-Peris, E., Gonzalvez-Macia, J., Corberan, J.M. (2017b). Evaluation of different heat pump systems for sanitary hot water production using natural refrigerants. *Applied Enerty, 190, 911-919.*

Pitarch, M., Navarro-Peris, E., Gonzalvez-Macia, J., Corberan, J.M. (2017c). Evaluation of optimal subcooling in subcritical heat pump systems. *International Journal of Refrigeration, 83, 18-31.*

Pottker, G. and P. S. Hrnjak, (2012). Potentials for COP increase in Vapor Compression Systems, ACRC TR 294. University of Illinois at Urbana-Champaign.

Pottker, G., Hrnjak, P. (2015a). Effect of the condenser subcooling on the performance of vapor compression system. *International Journal of Refrigeration, 50, 156-164.*

Pottker, G., Hrnjak, P. (2015b). Thermoeconomic optimization of subcooler and superheated vapor compression refrigeration cycle. *Energy, 31, 2108-2128.*

Selbas, R., Kizilkan, O., Sencan, A. (2006). Experimental investigation of the effect of condenser subcooling in R134a and R1234yf air conditioning systems with and without internal heat exchanger. *International Journal of Refrigeration, 50, 104-113.*

Xu, L., Hrnjak, P. (2014). Potential of Controlling Subcooling In Residential A/C System. *Proceedings of the International Refrigeration and Air Conditioning Conference at Purdue, West Lafayette*, *USA.* West Lafayette, USA (2387). Purdue University.

Xu, L. and P.S. Hrnjak, (2014). Potential of Controlling Subcooling in Residential Air Conditioning System ACRC TR311. University of Illinois at Urbana-Champaign.

Yamanaka, Y., Matsuo, H., Tuzuki, K., Tsuboko, T., 1997, Development of Sub-cool system, SAE Technical Paper Series, paper 970110.

ACKNOWLEDGEMENT

This work was supported by the Air Conditioning and Refrigeration Center at the University of Illinois at Urbana-Champaign. Support from ACRC members and sponsors are gratefully acknowledged.